Native T_1 Value in the Remote Myocardium Is Independently Associated With Left Ventricular Dysfunction in Patients With Prior Myocardial Infarction

Shiro Nakamori, MD,[1] Javid Alakbarli, MD,[1] Steven Bellm, MD,[1] Shweta R. Motiwala, MD,[1] Gifty Addae, BS,[1] Warren J. Manning, MD,[1,2] and Reza Nezafat, PhD[1]*

Purpose: To compare remote myocardium native T_1 in patients with chronic myocardial infarction (MI) and controls without MI and to elucidate the relationship of infarct size and native T_1 in the remote myocardium for the prediction of left ventricular (LV) systolic dysfunction after MI.
Materials and Methods: A total of 41 chronic MI (18 anterior MI) patients and 15 age-matched volunteers with normal LV systolic function and no history of MI underwent cardiac magnetic resonance imaging (MRI) at 1.5T. Native T_1 map was performed using a slice interleaved T_1 mapping and late gadolinium enhancement (LGE) imaging. Cine MR was acquired to assess LV function and mass.
Results: The remote myocardium native T_1 time was significantly elevated in patients with prior MI, compared to controls, for both anterior MI and nonanterior MI (anterior MI: 1099 ± 30, nonanterior MI: 1097 ± 39, controls: 1068 ± 25 msec, $P < 0.05$). Remote myocardium native T_1 moderately correlated with LV volume, mass index, and ejection fraction ($r = 0.38$, 0.50, –0.49, respectively, all $P < 0.05$). LGE infarct size had a moderate correlation with reduced LV ejection fraction ($r = –0.33$, $P < 0.05$), but there was no significant association between native T_1 and infarct size. Native T_1 time in the remote myocardium was independently associated with reduced LV ejection fraction, after adjusting for age, gender, infarct size, and comorbidity ($\beta = –0.34$, $P = 0.03$).
Conclusion: In chronic MI, the severity of LV systolic dysfunction after MI is independently associated with native T_1 in the remote myocardium. Diffuse myocardial fibrosis in the remote myocardium may play an important pathophysiological role of post-MI LV dysfunction.
Level of Evidence: 1.

J. MAGN. RESON. IMAGING 2017;00:000–000.

Left ventricular (LV) systolic dysfunction after myocardial infarction (MI) is a major cause of symptomatic heart failure and thought to be an important aspect of mortality.[1,2] The prophylactic use of primary prevention implantable cardioverter-defibrillator for reducing mortality due to ventricular arrhythmias is widely accepted in patients with heart failure and a low left ventricular ejection fraction (LVEF).[3,4] However, the importance of LV dysfunction as a pathogenic mechanism after MI is incompletely understood.

Following MI, cardiac magnetic resonance (MR) studies have focused on the assessment of the infarcted tissue.[5–8] Native T_1 mapping is a noninvasive cardiac MR biomarker for the assessment of diffuse myocardial fibrosis, and area where late gadolinium enhancement (LGE) cardiac MR has limited accuracy[9,10] and may detect reactive fibrosis in the noninfarcted myocardium. In human as well as animal models of post-MI remodeling, fibroblast stimulation has been shown to cause extracellular volume expansion of both

View this article online at wileyonlinelibrary.com. DOI: 10.1002/jmri.25652

Received Nov 11, 2016, Accepted for publication Jan 12, 2017.

*Address reprint requests to: R.N., Department of Medicine, Cardiovascular Division, Beth Israel Deaconess Medical Center, 330 Brookline Ave., Boston, MA 02215. E-mail: rnezafat@bidmc.harvard.edu

From the [1]Department of Medicine (Cardiovascular Division), Beth Israel Deaconess Medical Center and Harvard Medical School, Boston, Massachusetts, USA; and [2]Department of Radiology, Beth Israel Deaconess Medical Center and Harvard Medical School, Boston, Massachusetts, USA

TABLE 1. Clinical Characteristics of the Study Population

Characteristics	Control subjects ($n = 15$)	Chronic MI patients ($n = 41$)	P value
Age (years)	62 ± 8	63 ± 9	0.57
Male (%)	8 (53)	30 (73)	0.16
BMI (kg/m^2	24.0 ± 3.2	27.4 ± 4.9	0.017
Hypertension (%)	3 (20)	15 (37)	0.24
Systolic blood pressure (mmHg)	123 ± 19	120 ± 18	0.51
Diastolic blood pressure (mmHg)	72 ± 13	70 ± 12	0.57
Heart rate (beats/min)	67 ± 10	68 ± 14	0.74
Diabetes mellitus (%)	3 (20)	13 (32)	0.39
Hypercholesteloremia (%)	5 (33)	14 (34)	0.96
Current smoking (%)	1 (7)	8 (20)	0.25
BMI ≥ 30 (%)	1 (7)	10 (24)	0.14
Medication			
Aspirin	0 (0)	41 (100)	<0.001
ACEi/ARB	0 (0)	35 (85)	<0.001
Beta-blocker	3 (20)	38 (93)	<0.001
Aldosterone-receptor antagonists	0 (0)	12 (29)	0.018
Statin	5 (33)	36 (88)	<0.001
NYHA functional class (I/II/III/IV)	—	12/27/2/0	—
Anterior MI (%)	—	18 (44)	—
Primary PCI (%)	—	22 (54)	—
Age of infarct (years)	—	5 (1—15)	—

Variables given are mean ± SD or N (%) or median (interquartile range).
ACEi = angiotensin-converting enzyme inhibitors; ARB = angiotensin-receptor blockers; BMI = body mass index; MI = myocardial infarction NYHA = New York Heart Association; PCI = percutaneous coronary intervention.

the infarcted and the noninfarcted myocardium,[11,12] and studies have reported on native T_1 during the acute phase of MI.[13,14] However, heart failure is more common in chronic MI[15] and the association between native T_1 and LV function/geometry in chronic MI remains to be fully clarified. We hypothesized that diffuse myocardial fibrosis of the remote noninfarcted area would be associated with progressive deterioration of LV systolic function.

Materials and Methods

We prospectively recruited 41 consecutive patients (30 male, mean age; 63 years) with prior MI (18 anterior MI) and 15 age-matched control subjects with normal LV systolic function, no symptoms of heart failure or MI, and no other cardiovascular diseases. The severity of heart failure was assessed based on the New York Heart Association (NYHA) Class guidelines.[16] All participants were in sinus rhythm at the time of the scan. The study protocol was approved by our Institutional Review Board. Written informed consent was obtained from all subjects. Imaging was performed on a 1.5T MRI scanner (Achieva, Philips Medical Systems, Best, Netherlands) equipped with a 32-element cardiac-surface coil. The protocol included cine cardiac MR and native T_1 map, followed by LGE. To assess LV/right ventricular myocardial function, geometry and mass, 10–12 short-axis stack images, and 4-chamber cines were acquired using a breath-hold, electrocardiogram (ECG)-gated steady-state free precession sequence (slice thickness, 8 mm; gap, 2 mm, in-plane spatial resolution 2 × 2 mm, 30 msec temporal resolution). Native T_1 map was acquired using an ECG-triggered, free-breathing slice-interleaved T_1 (STONE) sequence which enables acquisition of five slices in the short-axis plane within 90 seconds (repetition time / echo time [TR/TE] = 2.8/1.4 msec, flip angle = 70°, field of view [FOV] = 360 × 351 mm, voxel size = 2.1 × 2.1 mm, slice thickness = 8 mm, turbo field echo [TFE] factor = 86, SENSE factor = 2).[17] Then 10–20 minutes after injection of 0.1–0.2 mmol/kg of Gd-DTPA (Magnevist; Bayer Schering, Berlin, Germany) or Gd-BOPTA (MultiHance; Bracco Imaging, Milan, Italy), short- and long-axis inversion recovery LGE images were acquired with a 3D phase sensitive inversion recovery sequence (PSIR) (5-mm slice thickness, TR/TE = 5.3/2.1 msec, flip angle = 70°, FOV = 320 × 320 × 125 mm, acquisition matrix = 224 × 224 × 23 and spatial resolution = 1.4 × 1.4 × 1.5 mm). Cardiac MR images

TABLE 2. Clinical Characteristics of the Study Population

Characteristics	Control subjects ($n = 15$)	Chronic MI patients ($n = 41$)	P value
LV EDV (ml)	114.9 ± 23.1	210.8 ± 63.5	<0.001
LV EDV index (ml/m^2	66.8 ± 10.1	107.9 ± 29.8	<0.001
LV ESV (ml)	44.6 ± 10.4	132.5 ± 55.8	<0.001
LV ESV index (ml/m^2	25.9 ± 5.1	68.4 ± 29.0	<0.001
LV stroke volume (ml)	70.3 ± 13.9	78.2 ± 24.3	0.24
LV ejection fraction (%)	61.3 ± 3.4	38.4 ± 11.0	<0.001
LV mass (g)	65.9 ± 14.6	118.1 ± 31.0	<0.001
LV mass index (g/m^2	38.3 ± 6.4	60.6 ± 15.3	<0.001
LV mass/ LV EDV (g/ml)	0.58 ± 0.10	0.59 ± 0.18	0.92
Sphericity index	0.49 ± 0.12	0.55 ± 0.16	0.21
LVDd (short axis) (mm)	47.7 ± 4.0	57.3 ± 7.5	<0.001
LV length (4 chamber) (mm)	76.9 ± 6.6	90.7 ± 9.6	<0.001
RV EDV (ml)	119.3 ± 24.0	133.2 ± 41.1	0.22
RV EDV index (ml/m^2	69.3 ± 10.5	67.7 ± 17.4	0.74
RV ESV (ml)	48.6 ± 13.3	59.1 ± 27.7	0.06
RV stroke volume (ml)	70.7 ± 14.9	74.1 ± 21.9	0.58
RV ejection fraction (%)	59.5 ± 6.0	56.7 ± 10.5	0.33
LGE, n (%)	0 (0%)	41 (100%)	<0.001
Infarct size (g)	—	13.2 ± 7.6	—
Infarct size/ LV mass (%)	—	11.6 ± 6.6	—
Average remote T_1 (msec)	1068 ± 25	1098 ± 35	0.003
Remote T_1 in apical slice (msec)	1079 ± 28	1107 ± 40	0.02
Remote T_1 in mid slice (msec)	1056 ± 31	1096 ± 37	<0.001
Remote T_1 in basal slice (msec)	1075 ± 32	1094 ± 42	0.11

Variables given are mean ± SD or N (%).
LV = left ventricular; EDV = end-diastolic volume; ESV = end-systolic volume; RV = right ventricular; LGE = late gadolinium enhancement; Dd = diastolic diameter.

were analyzed using a commercial workstation (Extend MR WorkSpace, v. 2.3.6.3, Philips Healthcare). At end-diastole, epi- and endocardial LV borders were manually traced in contiguous short-axis cine images covering the apex to mitral valve plane to calculate LV mass and end-diastolic volume (EDV) and endo of end-systole to end-systolic volume (ESV), stroke volume, and ejection fraction (EF). LV mass was calculated as the sum of the myocardial volume multiplied by the specific gravity (1.05g/mL) of myocardial tissue.[18] Sphericity index was calculated as the ratio of the LV diastolic volume to the volume of a sphere with the diameter of the long axis of the LV in diastole obtained from a 4-chamber cine image (LV volume/[LV long axis length$^3 \times \pi/6$]), using a commercial workstation (OsiriX environment, Pixmeo, Geneva, Switzerland).[19,20] Short-axis slices of native T_1 mapping images were analyzed using custom software (MediaCare, Boston, MA). The T_1 map of each scan was estimated by voxelwise curve fitting using a 2-paramter fit model. Motion correction was performed using the adaptive registration of varying contrast-weighted images for improved tissue characterization (ARCTIC).[21] In this study the remote myocardium measurements relied on visually identifying the normal area on the corresponding LGE image. For each short-axis cross-section, after the endocardial and epicardial borders were traced a region of interest (ROI) was placed on myocardium without enhancement on the LGE image and standardized to be of similar size and shape with a relatively large size of 150 pixels or greater, by avoiding contamination with signal from the blood pool and artifact due to a misregistration error. The native T_1 value of the noninfarct remote myocardium in patients with prior MI were calculated as an average ROI value on the three mid-ventricular slices. Native myocardial T_1 in control subjects were measured over the three mid-ventricular slices by manually drawing epicardial and endocardial contours. To evaluate interobserver reproducibility, measurements of LV native T_1 from 10 random patients with prior MI were independently assessed by two observers (S.N., with 7 years of experience, and J.A., with 2 years of experience). One of the two observers measured LV native T_1 twice on 2 separate

days with a washout period of at least 2 weeks to assess intraobserver reproducibility. In 30 MI patients with hematocrit assessment on the day of scanning, T_1 values of remote myocardium and LV blood pool were similarly determined, before and after contrast injection. Then extracellular volume fraction was calculated according to the formula as:

$$\text{Extracellular volume fraction} = (1\text{-hematocrit}) \times \{[(1/T_1\text{myocardium.post})\text{-}(1/T_1\text{myocardium.pre})] [(1/T_1\text{blood.post})\text{-}(1/T_1\text{blood.pre})]\} \times 100(\%)$$

On LGE images, the presence or absence of LGE was visually assessed by two experienced cardiologists (S.N., with 7 years of experience, and S.R.M., with 3 years of experience). If LGE was present, the quantitative extent of hyperenhancement was manually traced and infarct size was expressed as a percent of total LV mass and as a total volume. Infarct regions with evidence of microvascular obstruction were included within the infarct area.

Statistical analyses were performed using SPSS v. 19 software (IBM, Armonk, NY) and MedCalc for Windows (v. 14.8.1, Ostend, Belgium). Continuous variables are expressed as mean ± standard deviation (SD) or median [quartiles] if not normally distributed, and compared using an unpaired Student's *t*-test or Mann–Whitney nonparametric test as appropriate. Significance of difference of native T_1 time among the three groups were evaluated by one-way analysis of variance (ANOVA) with Bonferroni's post-hoc test. Categorical variables are reported as counts and percentages, and compared using a chi-square test. All tests were two-sided and $P < 0.05$ was considered statistically significant. Depending on data distribution, either a Pearson or Spearman correlation coefficient was calculated to investigate possible associations of continuous outcome measures. Skewed distributions were logarithmically transformed before regression analysis. Multivariate stepwise regression analyses with several potentially confounding factors were performed with LVEF as the dependent variable. Intra- and interobserver of T_1 times in the remote myocardium were assessed with Bland–Altman methods and intraclass correlation coefficient.

Results

Baseline clinical characteristics of the controls and chronic MI groups are summarized in Table 1. The mean age of all subjects was 63 years (range 40–81). Chronic MI patients were more frequently male, obese, and had a higher body mass index, while both groups had similar history of hypertension, diabetes mellitus, dyslipidemia, and current smoking. Two-thirds of chronic MI patients reported exertional dyspnea, predominantly NYHA Functional class II. Table 2 summarizes cardiac MR findings of the two groups. Chronic MI patients had significantly bigger LV mass index, higher LV ED and ES volumes, and lower LVEF (all $P < 0.001$). LGE hyperenhancement was observed in all chronic MI patients: transmural LGE in 13 patients, and subendocardial LGE in 28 patients. The mean infarct size was 13.2 ± 7.6 g and 12% of total LV myocardium, indicating relatively small infarctions. The mean remote myocardium native T_1

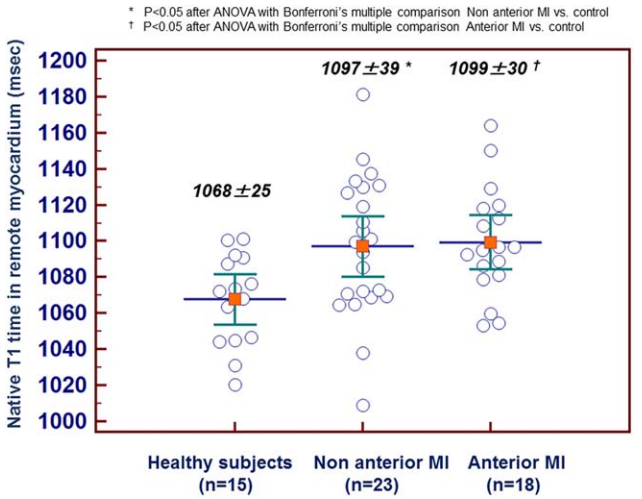

FIGURE 1: Comparison of native remote myocardium T_1. Native T_1 time was significantly elevated in patients with chronic myocardial infarction in comparison to healthy control subjects. There was no significant difference in native T_1 time between anterior MI vs. nonanterior MI.

was significantly higher in patients with prior MI compared with that in controls ($P = 0.003$). Even after subclassified into anterior MI ($n = 18$) and nonanterior MI ($n = 23$), the mean remote myocardium native T_1 was significantly higher in both MI groups than that in control subjects (anterior MI: 1099 ± 30, nonanterior MI: 1097 ± 39, and controls: 1068 ± 25 msec, $P < 0.05$ after Bonferroni correction, respectively). There was no significant difference in the native T_1 value of remote myocardium between anterior MI vs. nonanterior MI groups (Fig. 1). Figure 2 shows the representative cases from chronic anterior MI with and without increased remote myocardium native T_1. Compared to the case without increased remote native T_1 (Fig. 2a), the case with increased native remote T_1 (Fig. 2b) demonstrated severe LV systolic dysfunction with mild hypertrophy in the remote myocardium despite similar transmural infarct and smaller infarct size. Figure 3 shows the relationship between remote myocardium native T_1 and LV volumes, mass, and EF. There was a moderate positive correlation with LV mass index ($r = 0.50$, $P < 0.001$), LV EDV index ($r = 0.38$, $P = 0.004$), LV ESV index ($r = 0.45$, $P = 0.001$), and negative correlation with LVEF ($r = -0.49$, $P < 0.001$). Remote myocardium native T_1 value also had univariate association with the presence of any MI ($\beta = 0.39$, $P = 0.003$) as well as LV dysfunction. There were no significant correlations between remote myocardium native T_1 and LV spherical geometry or infarct size (Table 3). Table 4 shows the univariate coefficients between reduced LVEF, patient characteristics, and cardiac MR parameters and multiple stepwise regression analysis investigating the relationship between reduced LVEF with clinical characteristics and cardiac MR findings in chronic MI subjects. On multivariable analysis that included age, gender, and variables with $P < 0.15$ in

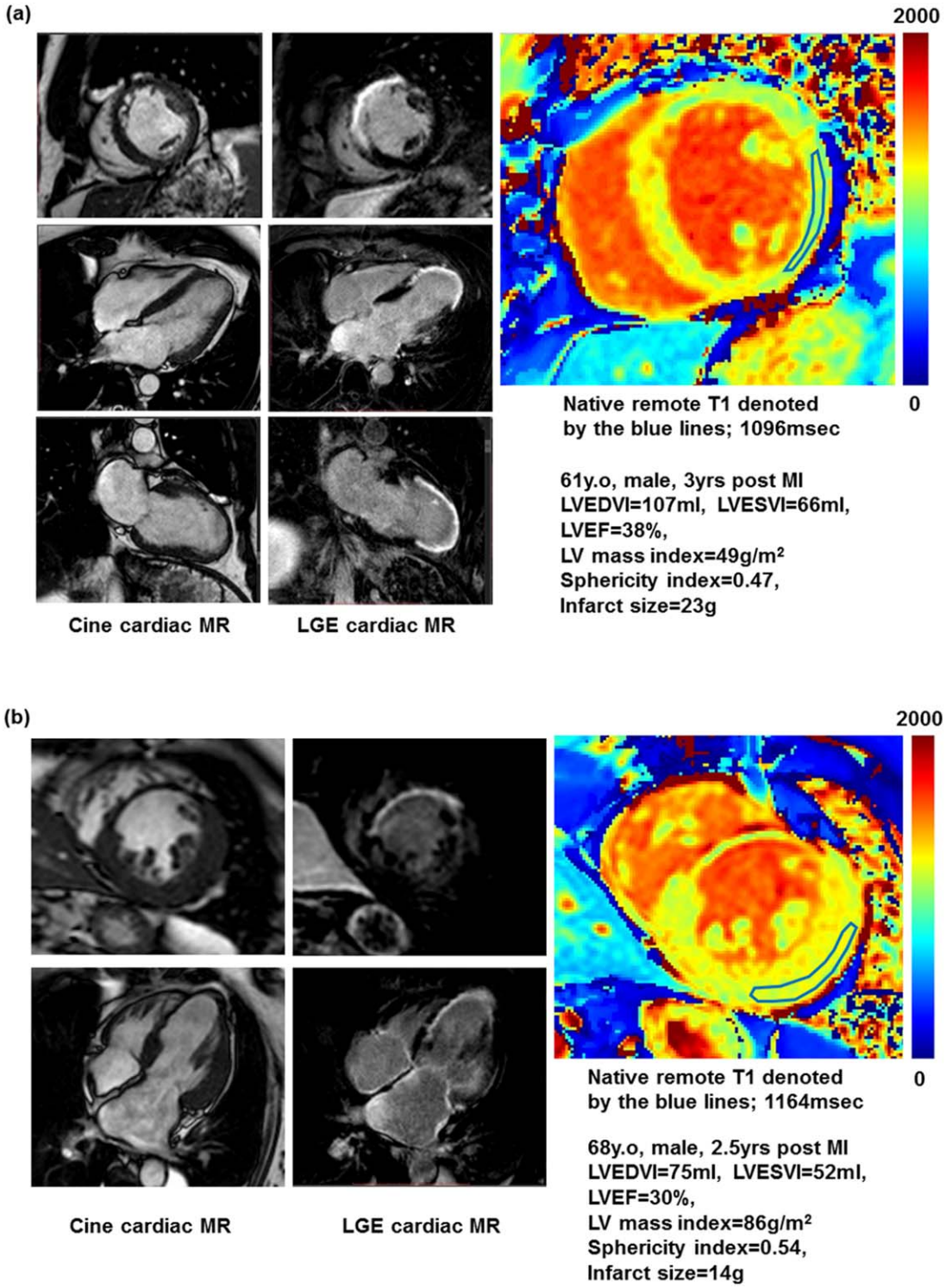

FIGURE 2: Representative cases with myocardial infarction. Example cases (a) 61-year-old, 3 years postanteroseptal myocardial infarction and remote T_1 of 1096 msec. Moderate LV systolic dysfunction was documented with mildly dilated LV volume and thinning of the mid and distal anteroseptal wall and apex. LGE image by cardiac MR showed transmural enhancement in the mid and distal septum, anterior wall and apex. (b) 68-year-old, 2.5 years post-similar anteroseptal myocardial infarction and high remote T_1 of 1164 msec. LGE infarct was transmural, but infarct size was relatively smaller than that of case A on LGE images. There was severe LV systolic dysfunction with mild hypertrophy in the remote myocardium.

the univariate analysis, the native T_1 values in the remote myocardium were independent predictors of reduced LVEF ($\beta = -0.34$, $P = 0.03$). Although infarct size showed significant univariate association with reduced LVEF, this relationship was no longer significant with multivariable analysis (Table 5). In 30 of 41 MI patients with extracellular volume fraction data, remote extracellular volume fraction appeared more likely to be similarly and moderately

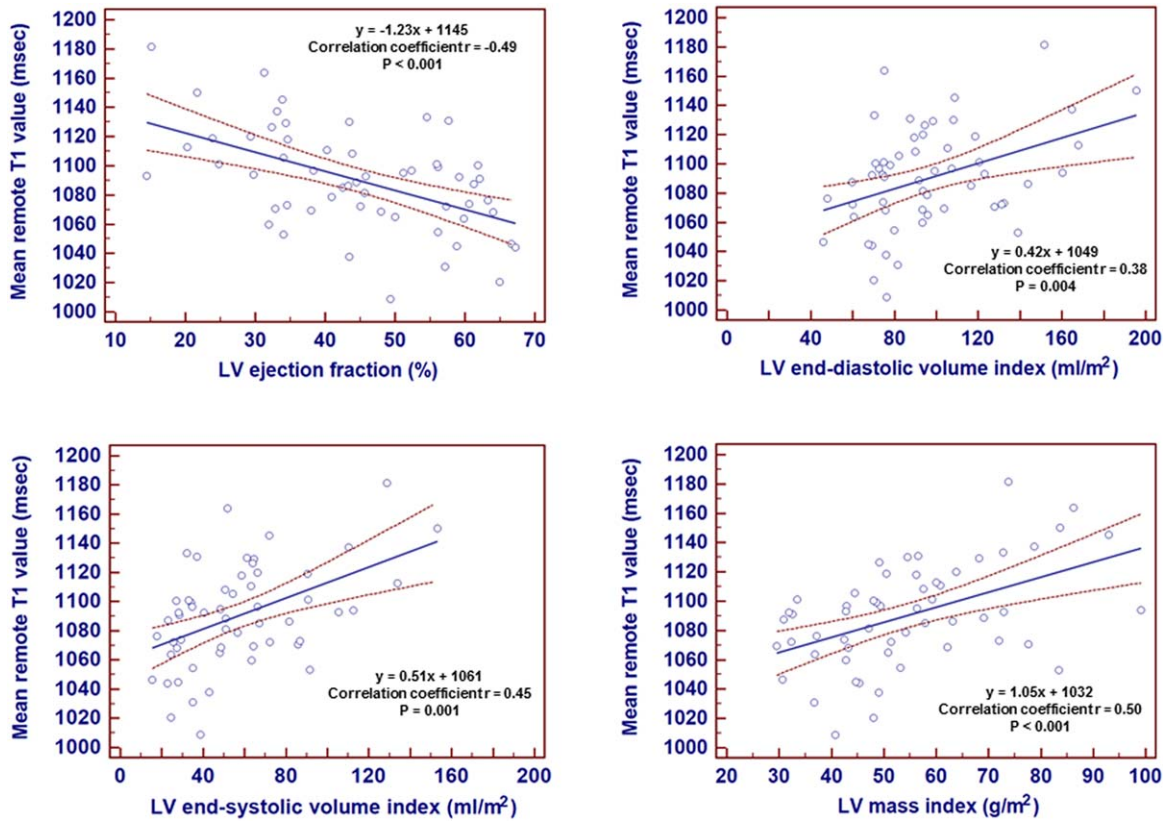

FIGURE 3: Correlation between native remote T_1 value and LV volumes, mass, and ejection fraction. Remote native T_1 time was moderately correlated with LV (a) ejection fraction, (b) end-diastolic volume index, (c) end-systolic volume index, and (d) LV mass index.

associated with reduced LVEF ($r = -0.32$, $P = 0.085$). The intraclass coefficients (ICC) for interobserver and intraobserver measurements of native remote myocardial T_1 were 0.88 (95% confidence interval [CI]: 0.72–0.94) and 0.91 (95% CI: 0.82–0.96), respectively. Bland–Altman analysis revealed acceptable agreement with a mean difference of 0.8% (95% CI; 0.2%–1.5%) and –0.6% (95% CI; –1.1%–0%) for inter- and intraobserver measurements, respectively.

Discussion

The present study demonstrated that 1) native remote myocardium T_1 is elevated in patients with prior MI compared with age-matched controls; 2) native remote myocardium T_1 and infarct size have similarly moderate correlation with reduced LVEF; and 3) in multivariate analysis, native T_1 independently correlates well with reduced LVEF beyond infarct. To the best of our knowledge, this is the first study to assess native remote myocardium T_1 in chronic MI patients using a slice interleaved T_1 mapping sequence (STONE) and to compare native remote myocardium T_1 with infarct size against LV dysfunction in the chronic phase after MI.

A diffuse myocardial fibrosis is a marker for subclinical disease, a fundamental feature of myocardial remodeling,[22] an independent predictor of adverse cardiovascular events,[23,24] and a potential target for medical interventions. Despite the importance of this measure of diffuse myocardial fibrosis, previous reports of post-MI remodeling were based on studies in infarct size and clinical findings.[25,26] Several investigators recently attempted to elucidate myocardial tissue characterization in the remote myocardium by using noninvasive T_1 mapping. In a study by Carrick et al, native remote myocardium T_1 predicted LV adverse remodeling in patients with acute MI.[14] However, T_1 mapping was acquired in the acute MI phase, without comparison of its diagnostic utility in the chronic phase with LV dysfunction. Native remote myocardium T_1 in the acute phase theoretically mirror the extent of myocardial edema as well as extracellular volume expansion and does not necessarily have a strong correlation with histological fibrosis in the chronic phase. Therefore, an increased native remote myocardium T_1 value shortly after MI may represent the initiation of diffuse fibrosis, as suggested by prior animal studies. In addition, our observations are similar to Chan et al that postcontrast remote myocardium T_1 is shorter in both patients with subacute and chronic MI.[13]

In contrast to the studies of Anversa et al[27] and Rumberger et al,[26] which found that the magnitude of post-MI LV systolic dysfunction is related to infarct size, we found that the native remote T_1 value was associated with LV

TABLE 3. Univariate Regression Analysis Between Native T_1 in Remote Myocardium in All Subjects ($n = 56$)

	beta (95% CI for the coefficient)	*P* value
Patient characteristics		
Age	0.01 (−1.01, 1.09)	0.94
Gender	0.19 (−5.29, 33.21)	0.15
Body mass index	−0.05 (−2.41, 1.66)	0.71
Systolic blood pressure	−0.28 (−1.07, −0.03)	0.039
Heart rate	0.18 (−0.24, 1.18)	0.19
Hypertension	0.16 (−7.97, 32.18)	0.23
Diabetes mellitus	0.07 (−15.52, 26.43)	0.60
Any MI	0.39 (10.61, 50.18)	0.003
Primary PCI	−0.20 (−35.80, 8.10)	0.21
Infarct age	−0.19 (−2.35, 0.85)	0.34
CMR findings		
LV ejection fraction	−0.49 (−1.83, −0.64)	<0.001
LV end−diastolic volume index	0.38 (0.14, 0.70)	0.004
LV end-systolic volume index	0.45 (0.23, 0.78)	0.001
LV mass index	0.50 (0.56, 1.55)	<0.001
LV mass/ LV end-diastolic volume	0.18 (−20.24, 98.60)	0.19
Sphericity index	−0.05 (−74.23, 53.32)	0.74
RV ejection fraction	−0.17 (−1.61, 0.38)	0.22
RV end-diastolic volume index	−0.13 (−0.90, 0.31)	0.34
RV end-systolic volume	0.06 (−0.30, 0.46)	0.67
Infarct size, g	0.19 (−0.57, 2.37)	0.22
Infarct size, % LV mass	−0.01 (−1.75, 1.68)	0.97

Abbreviations as in Tables 1 and 2.

dysfunction beyond infarct size. Moreover, it should be noted that the elevated native remote myocardium T_1 was a powerful, independent predictor for reduced LVEF, even after taking potential confounders into consideration. These findings are consistent with previous animal and human studies[11,12,28,29] and suggest that post-MI LV dysfunction is related to diffuse myocardial fibrosis in the remote myocardium in patients with relatively small MI, which plays a pivotal role in the development, progression, and clinical manifestations of heart failure.

In a recent animal study of Kali et al,[30] native T_1 at 3T provided a similar diagnostic accuracy for detecting infarct location, size, and transmurality of chronic MI to LGE image. The present study demonstrated that the native T_1 method can be applicable for assessment of noninfarct remote myocardium mostly associated with post-MI LV remodeling. Considering this information not given by LGE image, shorter scan time, and noncontrast material requirement, the comprehensive native T_1 map approach has the potential for widespread clinical application and might improve outcomes in MI patient with chronic kidney disease.

Our study has several limitations. First, the present study is a single-center study of relatively small sample size. Second, traditional coronary risk factors potentially may contribute to the elevation of native remote myocardium T_1 value. However, given that fibroblast stimulation increases collagen synthesis and causes fibrosis of both the infarcted and noninfarcted myocardium after MI, the elevated native remote myocardium T_1 following MI could contribute to adverse LV remodeling.

In conclusion, LV systolic dysfunction in chronic MI is independently associated with diffuse myocardial fibrosis in the remote myocardium. The current results should alert the clinician to the potential coexistence of diffuse myocardial fibrosis in the remote myocardium. Larger, multicenter

TABLE 4. Univariate Regression Analysis Between LVEF in Chronic MI Patients ($n = 41$)

	beta (95% CI for the coefficient)	*P* value
Patient characteristics		
Age	0.07 (−0.30, 0.45)	0.68
Gender	0.21 (−2.59, 12.96)	0.19
Systolic blood pressure	0.32 (0.01, 0.40)	0.043
Hypertension	−0.24 (−12.56, 1.65)	0.13
Diabetes mellitus	−0.15 (−11.05, 3.92)	0.34
Anterior MI	0.03 (−6.37, 7.83)	0.84
Primary PCI	0.08 (−5.28, 8.81)	0.62
Medications		
ACEi/ARB	−0.18 (−15.19, 4.45)	0.28
Beta blocker	0.20 (−4.85, 21.67)	0.21
Aldosterone-receptor antagonist	−0.14 (−10.99, 4.36)	0.39
Statin	0.16 (−5.19, 16.07)	0.31
CMR findings		
Native T_1 in remote myocardium	−0.35 (−0.20, −0.02)	0.023
Infarct size, g	−0.36 (−1.01, −0.04)	0.034
Infarct size, % LV mass	−0.31 (−1.04, −0.01)	0.046

Abbreviations as in Tables 1 and 2.

TABLE 5. Multivariate Stepwise Analysis of Chronic MI Subjects with reduced LVEF as the Dependent Variables (n=41)

	β	SE	p-value
Native remote myocardium T_1, msec	−0.34	0.047	0.029

The clinical characteristics that were univariate predictors of LVEF that were also included in the multivariate model were age (p=0.65), male (p=0.051), systolic blood pressure (p=0.17), hypertension (p=0.26) and infarct size (g) (p=0.079).

studies are needed to further confirm whether these results represent a potential therapeutic target.

Acknowledgment

Contract grant sponsor: Mie University Foundation International (scholarship to S.N.); Contract grant sponsor: National Institutes of Health (NIH); contract grant numbers: R01EB008743, 1R21HL127650, 1R01HL129185, and AHA 15EIA22710040 (to R.N.)

We thank Beth Goddu, RT, Sophie Berg, RN, and Kraig Kissinger, RT, for performance of the CMR studies.

References

1. Sutton MG, Sharpe N. Left ventricular remodeling after myocardial infarction pathophysiology and therapy. Circulation 2000;101:2981–2988.
2. Cohn JN, Ferrari R, Sharpe N. Cardiac remodeling-concepts and clinical implications: a consensus paper from an international forum on cardiac remodeling. J Am Coll Cardiol 2000;35:569–582.
3. Buxton AE, Lee KL, Fisher JD, Josephson ME, Prystowsky EN, Hafley G. A randomized study of the prevention of sudden death in patients with coronary artery disease. N Engl J Med 1999;341:1882–1890.
4. Bardy GH, Lee KL, Mark DB, et al. Amiodarone or an implantable cardioverter-defibrillator for congestive heart failure. N Engl J Med 2005;352:225–237.
5. Kwong RY, Chan AK, Brown KA, et al. Impact of unrecognized myocardial scar detected by cardiac magnetic resonance imaging on event-free survival in patients presenting with signs or symptoms of coronary artery disease. Circulation 2006;113:2733–2743.
6. Orn S, Manhenke C, Anand IS, et al. Effect of left ventricular scar size, location, and transmurality on left ventricular remodeling with healed myocardial infarction. Am J Cardiol 2007;99:1109–1114.
7. Kwon DH, Halley CM, Carrigan TP, et al. Extent of left ventricular scar predicts outcomes in ischemic cardiomyopathy patients with significantly reduced systolic function; a delayed hyperenhancement cardiac magnetic resonance study. JACC Cardiovasc Imaging 2009;2:34–44.

8. Wu Y, Chan CW, Nicholls JM, Liao S, Tse HF, Wu EX. MR study of the effect of infarct size and location on left ventricular functional and microstructural alterations in porcine models. J Magn Reson Imaging 2009;29:305–312.
9. Iles L, Pfluger H, Phrommintikul A, et al. Evaluation of diffuse myocardial fibrosis in heart failure with cardiac magnetic resonance contrast-enhanced T1 mapping. J Am Coll Cardiol 2008;52:1574–1580.
10. Flett AS, Hayward MP, Ashworth MT, et al. Equilibrium contrast cardiovascular magnetic resonance for the measurement of diffuse myocardial fibrosis: preliminary validation in humans. Circulation 2010; 122:138–144.
11. Volders PG, Willems IE, Cleutjens JP, Arends JW, Havenith MG, Daemen MJ. Interstitial collagen is increased in the non-infarcted human myocardium after myocardial infarction. J Mol Cell Cardiol 1993;25:1317–1323.
12. Tsuda T, Gao E, Evangelisti L, Markova D, Ma X, Chu ML. Post-ischemic myocardial fibrosis occurs independent of hemodynamic changes. Cardiovasc Res 2003;59:926–933.
13. Chan W, Duffy SJ, White DA, et al. Acute left ventricular remodeling following myocardial infarction: coupling of regional healing with remote extracellular matrix expansion. JACC Cardiovasc Imaging 2012;5:884–893.
14. Carrick D, Haig C, Rauhalammi S, et al. Pathophysiology of LV remodeling in survivors of STEMI: inflammation, remote myocardium, and prognosis. JACC Cardiovasc Imaging 2015;8:779–789.
15. Velagaleti RS, Pencina MJ, Murabito JM, et al. Long-term trends in the incidence of heart failure after myocardial infarction. Circulation 2008;118:2057–2062.
16. Dolgin M, ed. Nomenclature and criteria for diagnosis of diseases of the heart and great vessels, 9th ed. Boston: Little Brown & Co; 1994:253–256.
17. Weingartner S, Roujol S, Akcakaya M, Basha TA, Nezafat R. Free-breathing multislice native myocardial T1 mapping using the slice-interleaved T1 (STONE) sequence. Magn Reson Med 2014;74:115–124.
18. Semelka RC, Tomei E, Wagner S, et al. Normal left ventricular dimensions and function: interstudy reproducibility of measurements with cine MR imaging. Radiology 1990;174:763–768.
19. Koilpillai C, Quinones MA, Greenberg B, et al. Relation of ventricular size and function to heart failure status and ventricular dysrhythmia in patients with severe left ventricular dysfunction. Am J Cardiol 1996; 77:606–611.
20. Mannaerts HF, van der Heide JA, Kamp O, Stoel MG, Twisk J, Visser CA. Early identification of left ventricular remodelling after myocardial infarction, assessed by transthoracic 3D echocardiography. Eur Heart J 2004;25:680–687.
21. Roujol S, Foppa M, Weingartner S, Manning WJ, Nezafat R. Adaptive registration of varying contrast-weighted images for improved tissue characterization (ARCTIC): Application to T1 mapping. Magn Reson Med 2015;73:1469–1482.
22. Weber KT, Brilla CG. Pathological hypertrophy and cardiac interstitium. Circulation 1991;83:1849–1865.
23. Wong TC, Piehler K, Meier CG, et al. Association between extracellular matrix expansion quantified by cardiovascular magnetic resonance and short-term mortality. Circulation 2012;126:1206–1216.
24. Puntmann VO, Carr-White G, Jabbour A, et al. T1-mapping and outcome in nonischemic cardiomyopathy. JACC Cardiovasc Imaging 2016;9:40–50.
25. McKay RG, Pfeffer MA, Pasternak RC, et al. Left ventricular remodeling after myocardial infarction?: A corollary to infarct expansion. Circulation 1986;74:693–702.
26. Rumberger JA, Behrenbeck T, Breen JR, Reed JE, Gersh BJ. Nonparallel changes in global left ventricular chamber volume and muscle mass during the first year after transmural myocardial infarction in humans. J Am Coll Cardiol 1993;21:673–682.
27. Anversa P, Olivetti G, Capasso JM. Cellular basis of ventricular remodeling after myocardial infarction. Am J Cardiol 1991;68:7D–16D.
28. Beltrami CA, Finato N, Rocco M, et al. Structural basis of end-stage failure in ischemic cardiomyopathy in humans. Circulation 1994;89: 151–163.
29. Bishop JE, Greenbaum R, Gibson DG, Yacoub M, Laurent GJ. Enhanced deposition of predominantly type I collagen in myocardial disease. J Mol Cell Cardiol 1990;22:1157–1165.
30. Kali A, Cokic I, Tang RL, et al. Determination of location, size, and transmurality of chronic myocardial infarction without exogenous contrast media by using cardiac magnetic resonance imaging at 3 T. Circ Cardiovasc Imaging 2014;7:471–481.